Plasma Processes and Polymers
Article type: Full Paper

Title: **Young's modulus of plasma-polymerized allylamine films using micromechanical cantilever sensor and laser-based surface acoustic wave techniques**

Author(s), Corresponding Author(s)*

Masaya Toda*,
Tohoku University, 6-6-01 Aramaki-Aza-Aoba, Aoba-ku, Sendai 980-8579, Japan
E-mail: mtoda@nme.mech.tohoku.ac.jp

Koji Miyake,
National Institute of Advanced Industrial Science and Technology, 1-2-1 Namiki, Tsukuba, 305-8564, Japan

Li-Qiang Chu[a], Marjan Zakerin, Renate Förch[b], Rüdiger Berger*
Max Planck Institute for Polymer Research, Ackermannweg 10, Mainz D-55128, Germany

Akiko N. Itakura*
National Institute for Materials Science, 1-2-1 Sengen, Tsukuba 305-0047, Japan
E-mail: itakura.akiko@nims.go.jp

Abstract

Mechanical properties of ultra-thin organic films are of fundamental importance considering coating applications. Micromechanical cantilever sensor (MCS) and laser-based surface acoustic wave (LA-SAW) techniques were both used to measure the Young's moduli of plasma polymerized films at different humidities. For plasma polymerized allylamine (ppAA) films deposited at 5 W and 90 W, Young's moduli of 1400 ± 350 MPa and 110 ± 20 MPa at humidities between 10 – 40 %, and 1070 ± 250 MPa and 32 ± 10 MPa at humidities between 70 – 80 % were measured. LA-SAW technique revealed Young's moduli lower than 60 % of those by MCS technique. The difference suggests an enhanced swelling at the air interface or a gradient of cross-linking density. (120 words)

[a] Currently at Tianjin University of Science & Technology, No 29, 13th Avenue, TEDA, 300457 Tianjin, China. E-mail: chuliqiang@tust.edu.cn
[b] Currently at Eura Consult AG, Max-Eyth-Strasse 2, 73479 Ellwangen, Germany. E-mail: renate.foerch@euraconsult.de

1. Introduction

Organic thin films are an attractive approach to immobilize molecules [1-3] and to realize superhydrophobic [4, 5] and dielectric coatings. [6, 7] Organic thin films can be directly deposited on almost any substrate by using a plasma-assisted polymerization process. [8] In order to achieve efficient functionality of plasma polymerized organic thin films, specific organic molecules can be used during the deposition process. [9-11] In addition to the chemical functionality, the mechanical stability of plasma polymerized films plays a major role. For example, the coatings of mechanical components need to be highly resistant to wear, [12, 13] corrosion, [14, 15] and delamination. Plasma-assisted polymerization processes offer a unique option in thin film preparation, since the mechanical stability can be adapted by varying the deposition conditions. This in turn affects the cross-linking density and mobility of polymeric chains. [16] In general, it has been shown that films deposited at a higher input power level exhibit a higher cross-linking density. [17] Thereby Young's modulus, [18] hardness of film [19] and its wear resistance can be increased. [20]

Dynamic mechanical analysis (DMA) is a standard characterization method used to determine mechanical properties of polymers. However, DMA requires thick films (> 1µm) and is thus not appropriate for the study of thin (< 1µm) films. Nano-indentation technique is considered to be one of the most useful methods for determining Young's modulus (*E*) of thin films. [21-25] However, for ultra-thin films up to a thickness of 20 nm the indentation depth is limited to about 10 – 20 % of the film thickness. [26, 27] In other words, indentions of < 2 nm have to be made in order to avoid the influence of substrate materials. Such small indentations are possible by using scanning force microscopy methods. However, scanning force microscopy methods are able to sense local mechanical properties, which can be different to mechanical properties of entire film. Consequently, several measurements have to be performed at different positions. Mechanical properties of plasma-deposited films may vary according to their thickness.

Therefore, alternative methods have to be developed and evaluated to measure ultra-thin polymer films.

Recently, we described the possibility of calculating *E* of polymer films made by layer-by-layer deposition of polyelectrolytes (≤ 20 nm thickness) on the micromechanical cantilever sensor (MCS). [28-35] The swelling of polymer films in a solvent vapor environment transduces into a measurable bending of MCS. [36, 37] In this way, E of the thin polymer film can be calculated by determining the magnitude of bending and the swelling ratio. This method should in theory, be applicable for ultra-thin films made by plasma deposition.

Alternatively, *E* of ultra-thin films can be determined by laser-based surface acoustic wave (LA-SAW) technique. [38-41] Here, a surface acoustic wave (SAW) is generated by laser irradiation on top of the ultra-thin film. The phase velocity of SAW is dependent on *E*. Typically, LA-SAW technique performs well for ultra-thin films with a E > 300 GPa. [24] However, it is an open question whether thin polymer films can be measured using LA-SAW technique, and whether it is reliable in the case of ultra-thin plasma polymerized films.

In this study we used plasma polymerized allylamine (ppAA) as a model material. [42] The ppAA films deposited on MCS swell upon exposure to humidity, [37] and we have previously shown that the resulting changes in their mechanical properties can be measured by the bending of MCS. [43] Our current work focuses on calculating *E* of ultra-thin plasma polymerized films using (i) the bending characteristics of ppAA coated MCS, and (ii) LA-SAW propagation at surface in response to humidity changes. Ellipsometry was used to determine the material parameters additionally required for ppAA films to calculate *E*.

2. Experimental Section

I. Preparation of ppAA films

Allylamine monomer (99 %, Sigma-Aldrich) was plasma-polymerized with input power levels of 5 W and 90 W under continuous wave conditions, and a process pressure of 10 Pa. This

corresponds to our previous published experimental work using a 13.56 MHz Pyrex plasma reactor. [37, 42] The ppAA films deposited at a higher plasma power level (P = 90 W) resulted in a higher cross-linking density than those deposited at lower power level (P = 5 W). [23] Generally, films deposited at higher input power showed a higher roughness and cross-linking density [17]. The energetic ion bombardment and UV irradiation during the plasma deposition process determines the cross-linking density of the film. [44, 45]

II. Thickness measurement of ppAA films

Imaging ellipsometry (EP3, Nanofilm Technologie GmbH, Germany) was used to measure the thickness changes ($\Delta d/d$) of ppAA films under defined humidity conditions. The samples were mounted in the fluid cell (SL-cell, Nanofilm, volume 7 cm^3) with windows at an angle of 60° relative to the sample plane. A laser with a wavelength of 532 nm at an incident angle of 60° was used. For ellipsometric measurements, ppAA film was deposited directly onto a piece of silicon wafer ($n_{Si} = 3.879 - 0.0257i$). The refractive index of ppAA film, n_{ppAA}, was calculated from a fit to a model consisting of a single uniform layer on a substrate for each measurement. For a 5 W film of $n_{ppAA} = 1.564 - 0.0i$, and for a 90 W film of $n_{ppAA} = 1.624 - 0.0i$ resulted in the best fit. The errors of fits in both cases were $\pm$ 0.004. A scanning force microscope was used to measure the root mean square (RMS) surface roughness of ppAA films, which was 0.6 nm for a corresponding area of 1 μm^2.

III. Humidity (*H*) control

A humidity controller was used to control the partial vapor pressure in a fluid cell which enabled relative *H* conditions from 0 to 100 %. [46] In the dry state, the fluid cell was flushed with N_2 gas at a defined *H* by using a specially-constructed gas mass flow setup (flow controller: Model 80s, McMillan Company, Texas, USA). Different relative concentrations of N_2 and H_2O were obtained by mixing dry N_2 gas and N_2 gas saturated with water vapor at T = 20 °C. The setup

was operated at a constant flow speed of 0.5 L/min. After buffering the vapor, a small amount of the vapor was fed into the fluid cell by using an electric pump (NMP-30, Neuberger Inc., New Jersey, USA). For the measurements, a constant flow of 100 µL/min through the fluid cell was established (volume of the fluidic cell ~30 µL and volume of the connecting tubes ~20 µL). Given this set-up, the fluid cell environment changes between dry and different *H* states in desired steps of 10 %. After reaching the desired *H*, the system was flushed with dry N_2 and then the *H* was increased further.

IV. MCS bending measurement

The deflection and resonance frequency of MCS were measured by an optical beam deflection technique in the above-mentioned fluidic cell (SCENTRIS, VEECO Instruments, USA, **Figure 1**). We measured the resonant frequencies of eight MCSs arranged in a linear array. We used MCSs fabricated from Si with a thickness of 1.2 – 1.9 µm, a length of 500 µm, a width of 90 µm and a pitch of 250 µm (Octosensis, Micromotive GmbH, Germany). The resonant frequencies of uncoated MCS were 10730 ± 30 Hz and 6900 ± 20 Hz and were used for 5 W and 90 W ppAA coatings, respectively. The films of ppAA were prepared on the MCS chip and on Si wafer substrates in the same process described previously [42]. Each of the eight-MCS arrays had at least one MCS without a ppAA film (**Figure 1**). These were used as references and were required to compensate thermal drift in the setup that arises during a 24 h experiment.

3. Principle of Measurements

I. *E* calculation by MCS technique

Swelling of films deposited on MCS generates surface stress, which is proportional to the difference in expansion coefficients between the film and the substrate (**Figure 1**). [47] The deflection behavior of MCS can be described as being similar to the bending of a bi-metallic

strip upon temperature changes. [48] The change in deflection $\Delta\delta$ of a bi-material strip upon humidity changes ΔH is given by [49]

$$\Delta\delta = \frac{l^2}{2R} = \frac{3l^2 E_{\mathrm{Si}} E_{\mathrm{film}} t_{\mathrm{Si}} t_{\mathrm{film}} (t_{\mathrm{Si}} + t_{\mathrm{film}})}{(E_{\mathrm{Si}} {t_{\mathrm{Si}}}^2)^2 + (E_{\mathrm{film}} {t_{\mathrm{film}}}^2)^2 2E_{\mathrm{Si}} E_{\mathrm{film}} t_{\mathrm{Si}} t_{\mathrm{film}} (2{t_{\mathrm{Si}}}^2 + 3t_{\mathrm{Si}} t_{\mathrm{film}} + 2{t_{\mathrm{film}}}^2)} (\alpha_{\mathrm{film}} - \alpha_{\mathrm{Si}}) \Delta H \quad (1)\ ,$$

where α_{film} and α_{Si} are linear expansion coefficients of film and Si at a given *H*, E_{Si} and E_{film} are E of Si and film, t_{Si} and t_{film} are thicknesses of Si cantilever beam and film, l is a length of cantilever beam. The geometric values of l, t_{Si} and t_{film} are given by the fabrication design of MCS. Thus, α_{film} and E_{film} are the unknown parameters in equation (1). In order to check which magnitude of E_{film} values are accessible by this method, we calculated the change in deflection, $\Delta\delta$, at a typical α_{film} of 0.0001 for polymers for a ΔH of 10 % (**Figure 2**). For t_{film} < t_{Si} ($t_{\mathrm{film}}/t_{\mathrm{Si}}$ = 0.05), the deflection of MCS due to swelling of the film becomes almost directly proportional to E_{film} in the range of 10^7 – 10^{11} Pa. Typically, the deflection of MCS can be measured with an accuracy of < 1 nm. Thus E_{film} values of 10 MPa or more are accessible.

II. *E* calculation by LA-SAW technique:

Laser acoustic thin film analyzer (LA wave, IWS, Germany) was used to estimate *E* of thin ppAA films near the air surface. SAWs were generated by illumination of the surface with short laser pulses (wavelength: 337 nm, pulse duration of 0.5 ns, and power of 0.4 mW). This method is based on measuring the phase velocity of generated SAW. The SAW propagates along the surface of materials and its amplitude decays exponentially. In the case of thick bulk samples (homogeneous and isotropic materials without any film on top), the phase velocity c_{bulk} of SAW is given by equation (2) [50]

$$c_{\mathrm{bulk}} = \frac{0.87 + 1.12\nu^2}{1+\nu} \sqrt{\frac{E}{2\rho(1+\nu)}} \quad (2),$$

where v is Poisson ratio of a bulk sample material. Thus the phase velocity of SAW for bulk samples in the propagation direction depends on both E and ρ, and is, in particular, not related to the frequency of SAW. [51]

However, in the case of thin films on top of a bulk sample the depth of propagating SAW needs to be considered. The depth of propagating wave becomes proportional to wavelength [52] and decreases with diminishing frequency. Correspondingly, the phase velocity of SAW depends on the film's thickness and the frequency of SAW. [53] The phase velocity is, in particular, more relevant for thin films when the SAW is generated at a higher frequency. For a homogeneous and isotropic thin film and a homogeneous and isotropic substrate, the phase velocity $c_{\mathrm{film+substrate}}$ depends on E of the film and the substrate (E'_{film} and $E_{\mathrm{substrate}}$), on their Poisson's ratios (ν_{film} and $\nu_{\mathrm{substrate}}$), their densities (ρ_{film} and $\rho_{\mathrm{substrate}}$), the film thickness t, and the frequency of SAW , as represented by the dispersion relation, shown in the following equation (3).

$$c_{\mathrm{film+substrate}} = \mathrm{g}(E_{\mathrm{substrate}}, E_{\mathrm{film}}, \nu_{\mathrm{substrate}}, \nu_{\mathrm{film}}, \rho_{\mathrm{substrate}}, \rho_{\mathrm{film}}, t, f) \quad (3)$$

In our measurements, a pulsed nitrogen laser was used to generate a wide band surface wave. The laser beam was shaped into a line on sample surface by a cylindrical lens. The generated SAW impulses were detected by a transducer for at least two different distances, x_1 and x_2, from the transducer to the laser focus line. The surface wave velocity spectra $c(f)$ is obtained from:

$$c(f) = \frac{2\pi f(x_2 - x_1)}{[\phi_2(f,x_2) - \phi_1(f,x_1)]} \ , \quad (4)$$

where $\phi_1(f, x_1)$ and $\phi_2(f, x_2)$ are SAW phase values for frequency of f at positions x_1 and x_2, respectively. The $c(f)$ at a specific position can be obtained from a Fourier transformation of SAW signals in the time domain registered by the transducer at both distances. Then E'_{film} is obtained by fitting equation (4) to the dispersion data.

4. RESULTS

I. Vertical expansion: Thickness and swelling measurements

In order to calculate E_{film} by MCS method, the α_{film} at different H values of thin ppAA films were required. Here, we applied ellipsometry to determine the relative changes in the film thicknesses ($\Delta d/d$) of ppAA film at different H values (**Figure 3 (a)**). The ppAA films deposited in dry nitrogen at a plasma power level of 5 W and 90 W, had thicknesses of 86.4 $\pm$ 0.1 nm and 98.1 $\pm$ 0.4 nm, respectively. We found that the thickness of ppAA films increased linearly up to H = 60 %. In addition, the increase in thickness appeared to be independent of the plasma power level used until H = 60 % was reached. Thus, the H induced expansion coefficients were similar to the 5 W and 90 W ppAA films in the range of H = 0 % to H = 60 %. Above H = 60 %, the relative film thickness of 5 W deposited ppAA thin film increased significantly more than 90 W ppAA films. This difference in swelling was consistent with the assumption that 5 W ppAA films exhibit a lower cross-linking density and can thus incorporate more water molecules.

Since the ppAA film expansion was dependent on humidity, we calculated the corresponding humidity induced expansion coefficients, α, by H increments of 10 % (**Figure 3 (b)**). We obtained $\alpha_{film\perp}$ = 0.0005 $\pm$ 0.0002 for the H range from 5 % to 60 % for both 5 W and 90 W films. At H > 60 %, $\alpha_{film\perp}$ becomes 0.0032 $\pm$ 0.0002 and 0.0012 $\pm$ 0.0004 for the 5 W and 90 W ppAA films, respectively. The error bars correspond to the standard deviation of measurements at seven different areas of the same sample. The symbol $\perp$ denotes that we measured thickness changes by ellipsometry.

However, for MCS technique the humidity induced expansion coefficients of ppAA films along MCS lengths (i.e. $\alpha_{film//}$) are required. For thin films that swell homogeneously and isotropically $\alpha_{film//} = \alpha_{film\perp}$ can be assumed. Nevertheless, the ppAA film is anchored to the MCS surface. Thus, the presence of MCS surface hinders the lateral expansion of the ppAA

film and $\alpha_{film\,//} \leq \alpha_{film\,\perp}$. We will discuss errors in calculating E given this connection in section III-A.

II. Lateral Expansion: MCS bending measurement

Deflection of MCS by swelling ppAA films

Identical ppAA films were prepared on MCS and exposed to different H ranging from 0 % to 85 % using a computer-controlled setup (**Figure 4 (a) and (b))**. Two subsequent H cycles are plotted, showing the observed deflection for a 5 W ppAA film during both increasing and decreasing H cycles (**Figure 4 (a)**). One typical cycle of increasing and decreasing H for a 90 W ppAA film is shown in **Figure 4 (b)**. At time t = 10 minutes (**Figure 4(b)**) the stability of measured deflection signal was confirmed by keeping H = 20 % for a few hours. At constant H, fluctuations of deflections < 0.2 % were measured and were considered negligible. Furthermore, the drift of the entire setup was measured by determining the response of adjacent MCSs, acting as references that were not coated with a polymer film. The deflection values of such reference measurements were used to subtract background signals (**Supporting information**). Our measurements confirm reproducible swelling of ppAA films and indicate no significant or measurable polymer degradation during repeated exposure to humidity over the time frame studied in this experiment (30 hours).

Figure 4 (c) and (d) show the bending response of 5 W ppAA film and 90 W ppAA film over time for a stepwise H variation from 0 % to 10 %. After the exposure to each humid environment for 10 minutes (in steps of 1 %, 2.5 %, 5 %, and 10 %) the samples were exposed to dry N_2 for 20 minutes before the next exposure to humidity. By switching the single four-way valve we were able to create a dry condition in the sample chamber (**Figure 1**). For each dry exposure, the bending deflection returned to the initial zero point of deflection which confirmed that (i) the gas inside the chamber was replaced completely, and (ii) the reversible swelling of PPAA film (**Figure 4 (c) and (d))**.

It is worth to notice that the saturated deflection magnitude at the same H-level between the increasing and decreasing cycle is different. For example, at H = 10 % in the decreasing cycle the saturated deflection of 594 nm was measured. This value was slightly smaller than that deflection magnitude of 630 nm in the increasing cycle for a 5 W ppAA film. The hysteresis could be up to 6 % in deflection magnitude and indicates that the de-swelling of films was affected by remaining water molecules left over from previous humidity exposure to films.

Stress changes of swelling ppAA films

The change in stress within the swollen ppAA film can be calculated from the deflection magnitude of MCS using Stoney's formula. [54-56] Within the entire H range from 10 % to 80 %, we measured a larger stress change for the ppAA film deposited at 90 W compared with the one deposited at 5 W (**Figure 5).** Moreover, the experiments that were performed in the increasing H process showed a larger stress change compared to the subsequent experiments performed while reducing H. This behavior was found for both 5 W and 90 W ppAA films and was fully reproducible in the second cycle recorded the next day. At first glance, this additional water residue should lead to a higher stress magnitude while decreasing H, because more water was present in ppAA films. However, the presence of residual water also influences the E_{film}. Specifically, the presence of residual water decreases E of ppAA films. Consequently, the deflection magnitude and the calculated stress change both decrease compared to the experiment where H was increased stepwise. In order to address the overall changes in E_{film}, we calculated averaged stress changes (lines plotted in **Figure 5**). The results indicate an increase of the averaged stress change of the swollen ppAA film when exposed to humidity. However, the increase of averaged stress was not directly proportional to the level of H. At the highest measured level of H, the stress value for 90 W ppAA film was 1.6 times larger than that of 5 W ppAA film.

III. *E* calculations

A. MSC technique. We calculated E_{film} using equation (1) (circle symbols in **Figure 6**). For the calculation, the averaged deflections and calculated $\alpha_{\text{film}\perp}$ values based on ellipsometry data (**Figure 3 (b))** were used. Furthermore, in humid environments, the values of $\alpha_{\text{Si}} = 0$ and E_{Si} =165 GPa remained constant. However, it was important to consider the relationship of $\alpha_{\text{film}//} \leq \alpha_{\text{film}\perp}$ which was deduced from ellipsometry measurements. Therefore, our calculations of E_{film} using $\alpha_{\text{film}\perp}$ can be seen as the lower limits of E_{film}. In order to estimate an upper limit for E_{film}, the minimum swelling state of a ppAA film at a low *H* level was used. In the case of the small volume expansion, the effects from substrate can be disregarded. We determined that the swelling of ppAA film was isotropic and that the film expansion in both parallel (//) and vertical ($\perp$) directions was identical, i.e. 0.0005 for both of the ppAA films deposited at 5 W and 90 W (**Figure 3 (b)**).

Irrespective of the power level during plasma polymerization, E_{film} of both films decreased with increasing *H* (**Figure 6**). The E_{film} calculated for 5 W and 90 W ppAA films were 1070 $\pm$ 250 MPa and 1400 $\pm$ 350 MPa for H = 0 % and H = 10 % , respectively. These results were slightly lower than *E*-values obtained by nano-indentation on plasma-polymerized thin films of vinyltriethoxysilane (3 – 10 GPa [18]). We attribute the lower *E*-values for ppAA films to the different composition of films and their partially swollen state during measurements.

For H < 60 % almost no difference in E_{film} values between 5 W and 90 W ppAA films was found. For H > 60% the higher cross-linking density in 90 W film leads to a reduced swelling and thus to an increased E_{film} of 110 $\pm$ 20 MPa between H = 70 % and H = 80 % compared to 5 W film (32 $\pm$ 1 MPa). The results indicate that the mechanical properties vary less upon *H*-changes for a film with a higher crosslinking density, i.e. deposited at a higher power.

B. LA-SAW. LA-SAW measurement was performed over a $\boldsymbol{H}$ range of 20 – 50 % and at a room temperature of 25 ± 3 °C for ppAA films of thickness 100 ± 10 nm deposited on a Si-substrate. Then, SAW propagation along <011> direction of Si (100) was measured. SAWs with a frequency of 30 MHz were detected at different distances, $l + \Delta l$, where l was 25 mm and Δl was varied from 0 to 5 mm. The calculated phase velocity spectra of SAW wave–packets were used to fit $\boldsymbol{E'_{film}}$ of ppAA films (square symbols in **Figure 6**). $\boldsymbol{E_{substrate}}$ corresponds to Si substrate (density: 2.33 g/cm^3) and we took C_{11}: 165 GPa, C_{12}: 63.5 GPa, C_{44}: 79.6 GPa for each crystal orientation, respectively. X-ray reflectivity measurements (Rigaku RINT ATX-G) revealed a ppAA film density of 1.12 ± 0.06 g/cm^3 (5 W) and 1.55 ± 0.04 g/cm^3 (90 W). [57, 58] To determine the Poisson's ratio of films we are taking 0.4, which is a widely used value for polymers [59]. The $\boldsymbol{E'_{film}}$of the ppAA film of 5 W decreased from 0.249 GPa to 0.138 GPa for a H change from 15 % to 46 %. These $\boldsymbol{E'_{film}}$ values were 41 ± 38 % and 60 ± 30 % lower than ones calculated by MCS technique for 5 W ppAA and 90 W ppAA, respectively (**Figure 6)**. However, the relative differences of $\boldsymbol{E}$ between both films at different $\boldsymbol{H}$ levels were confirmed: The $\boldsymbol{E'_{film}}$ of the 90 W film was larger compared to the 5 W film, and the $\boldsymbol{E'_{film}}$ in high $\boldsymbol{H}$ conditions was smaller than in a low $\boldsymbol{H}$ environment.

6. Discussion

The E'_{film} in LA-SAW measurement was smaller compared to the E_{film} measurement using MCS technique. Based on surface acoustic waves, LA-SAW technique was more sensitive to polymer properties at its air interface and less sensitive to polymer properties at its substrate interface. The difference of calculated E'_{film} and E_{film} can be explained by two possible theories: (a) ppAA films swell more at polymer/air interface compared to the interface of solid substrate. The presence of substrate may even lead to some inhibition of swelling. (b) The crosslinking density of ppAA films was lower at the air-interface compared to its interface with

a solid substrate. In contrast, the driving force for cantilever bending occurs at the silicon substrate interface. We are of the opinion that both theories are feasible for ultra-thin ppAA films.

7. Conclusion and summary

We measured Young's modulus of approximately 100 nm thick polymerized films that were made using a plasma deposition process. We selected plasma-polymerized allylamine (ppAA) as model films that swell upon exposure to humidity. A decrease of Young's modulus with increasing H was consistently observed. The MCS technique is based on the measurement of the deflection of cantilever beams. The error of the measurement was dominated by the error of the expansion coefficient that was inferred from ellipsometry. In contrast, the LA-SAW technique revealed lower E values. We attribute this difference to a lower cross-linking density of ppAA films at the air interface, or to enhanced swelling of polymer close to the air interface.

One major outcome of this work is that both techniques MCS and LA-SAW are applicable for measuring ultra-thin plasma polymerized films and represent an alternative to nano-indentation measurements. Nano-indentation measurements might not be easily feasible in harsh environments such as polymer solvents. However, MCS technique is not only restricted to experiments involving humidity. It can be readily used in experiments using various polymer solvents and vapors. [46, 60, 61] A simple estimation revealed that MCS is able to measure E down to 10 MPa. In principle, the MCS method can be used to determine E for films with a thickness of less than 10 nm, as long as the expansion coefficient can be determined.

Acknowledgements:

We would like to thank Mr. Andrey Grinevich, who was an internship student from Charles University, and Dr. Megumi Fukuta from the National Institute of Advanced Industrial Science

and Technology for the measurements of LA-SAWs. Dr. Kenji Sakurai from NIMS is acknowledged for providing the X-ray refractivity tool and help in determining the film density. We acknowledge the input of our former group member Dr. Shin-ichi Igarashi (now at Shin-Etsu Chemical Co., Ltd.), as we started this research with him and the basic idea came from our discussions. This research was supported by funding from the Japanese Science and Technology Agency, National Institute for Material Science, and the Max Planck Institute for Polymer Research, Germany. We acknowledge partial financial support from the Deutsche Forschungsgemeinschaft (DFG) within the Strategic Japanese German Cooperative Program on Nanoelectronics (BE3286/2-1) and (BE 3286/4-1). In addition, we acknowledge the funding received from the Promotion of Joint International Research by the JSPS KAKENHI Grant Numbers 15KK0225.

Keywords: cantilever sensing, humidity sensor, plasma polymerization, Young's modulus of ultra-thin films

References

[1] Z. H. Zhang, Q. Chen, W. Knoll, R. Foerch, R. Holcomb, D. Roitman, *Macromolecules* **2003**, *36*, 7689.
[2] J. Homola, *Chem. Rev.* **2008**, *108*, 462.
[3] F. Rusmini, Z. Zhong, J. Feijen, *Biomacromolecules* **2007**, *8*, 1775.
[4] A. Lazauskas, J. Baltrusaitis, V. Grigaliūnas, D. Jucius, A. Guobienė, I. Prosyčevas, P. Narmontas, *Plasma Chem. Plasma Process.* **2013**, *34*, 271.
[5] A. Tuteja, W. Choi, M. Ma, J. M. Mabry, S. A. Mazzella, G. C. Rutledge, G. H. McKinley, R. E. Cohen, *Science* **2007**, *318*, 1618.
[6] Y. Xu, P. R. Berger, J. Cho, R. B. Timmons, *J. Electron. Mater.* **2004**, *33*, 1240.
[7] C. Reese, M. Roberts, M.-m. Ling, Z. Bao, *Mater. Today* **2004**, *7*, 20.
[8] E. Radeva, *Sensors and Actuators B: Chemical* **1997**, *44*, 275.
[9] L. Denis, D. Cossement, T. Godfroid, F. Renaux, C. Bittencourt, R. Snyders, M. Hecq, *Plasma Processes and Polymers* **2009**, *6*, 199.
[10] Y. Wang, J. Zhang, X. Shen, *Mater. Chem. Phys.* **2006**, *96*, 498.
[11] R. Morent, N. De Geyter, S. Van Vlierberghe, A. Beaurain, P. Dubruel, E. Payen, *Prog. Org. Coat.* **2011**, *70*, 336.
[12] H. Holleck, V. Schier, *Surf. Coat. Technol.* **1995**, *76-77*, 328.
[13] T. Spalvins, *Thin Solid Films* **1978**, *53*, 285.
[14] M. Stratmann, R. Feser, A. Leng, *Electrochim. Acta* **1994**, *39*, 1207.
[15] W. J. van Ooij, D. Zhu, M. Stacy, A. Seth, T. Mugada, J. Gandhi, P. Puomi, *Tsinghua Science and Technology* **2005**, *10*, 639.
[16] T. Kaule, Y. Zhang, S. Emmerling, S. Pihan, R. Foerch, J. Gutmann, H. J. Butt, R. Berger, U. Duerig, A. W. Knoll, *ACS Nano* **2013**, *7*, 748.
[17] Y. Zhang, J. Arfsten, S. A. Pihan, T. Kaule, R. Förch, R. Berger, *J. Colloid Interface Sci.* **2010**, *351*, 532.
[18] V. Cech, N. Inagaki, J. Vanek, R. Prikryl, A. Grycova, J. Zemek, *Thin Solid Films* **2006**, *502*, 181.
[19] J. Ahmad, K. Bazaka, M. Jacob, *Electronics* **2014**, *3*, 266.
[20] R. Berger, Y. Cheng, R. Förch, B. Gotsmann, J. S. Gutmann, T. Pakula, U. Rietzler, W. Schartl, M. Schmidt, A. Strack, J. Windeln, H. J. Butt, *Langmuir* **2007**, *23*, 3150.
[21] J. Domke, M. Radmacher, *Langmuir* **1998**, *14*, 3320.
[22] K. Miyake, N. Satomi, S. Sasaki, *Appl. Phys. Lett.* **2006**, *89*, 031925.
[23] S. Igarashi, A. N. Itakura, M. Kitajima, A. N. Chifen, R. Foerch, R. Berger, *Appl. Phys. Lett.* **2006**, *88*, 143119.
[24] T. Chudoba, M. Griepentrog, A. Dück, D. Schneider, F. Richter, *J. Mater. Res.* **2011**, *19*, 301.
[25] V. Cech, J. Lukes, E. Palesch, T. Lasota, *Plasma Processes and Polymers* **2015**, *12*, 864.
[26] H. J. Butt, B. Cappella, M. Kappl, *Surf. Sci. Rep.* **2005**, *59*, 1.
[27] D. Passeri, M. Rossi, E. Tamburri, M. L. Terranova, *Analytical and Bioanalytical Chemistry* **2012**, *405*, 1463.
[28] M. Toda, Y. Chen, S. K. Nett, A. N. Itakura, J. Gutmann, R. Berger, *Journal of Physical Chemistry C* **2014**, *118*, 8071.
[29] J. H. He, J. K. Luo, H. R. Le, D. F. Moore, *Materials Science and Engineering: A* **2006**, *423*, 134.
[30] G. J. McShane, M. Boutchich, A. S. Phani, D. F. Moore, T. J. Lu, *J Micromech Microeng* **2006**, *16*, 1926.
[31] S. He, J. S. Chang, L. Li, H. Ho, *Sensors and Actuators A: Physical* **2009**, *154*, 149.
[32] J. H. Lim, M. M. Ratnam, I. A. Azid, D. Mutharasu, *Optics and Lasers in Engineering* **2011**, *49*, 1301.

[33] I. Stachiv, D. Vokoun, Y.-R. Jeng, *Appl. Phys. Lett.* **2014**, *104*, 083102.
[34] S. Singamaneni, M. E. McConney, M. C. LeMieux, H. Jiang, J. O. Enlow, T. J. Bunning, R. R. Naik, V. V. Tsukruk, *Adv. Mater.* **2007**, *19*, 4248.
[35] J. H. He, J. K. Luo, H. R. Le, D. F. Moore, *Mat Sci Eng a-Struct* **2006**, *423*, 134.
[36] C. Ishiyama, Y. Higo, *J Polym Sci Pol Phys* **2002**, *40*, 460.
[37] S. Igarashi, A. N. Itakura, M. Toda, M. Kitajima, L. Chu, A. N. Chifene, R. Förch, R. Berger, *Sensors and Actuators B-Chemical* **2006**, *117*, 43.
[38] X. Xiao, X. M. Shan, Y. Kayaba, K. Kohmura, H. Tanaka, T. Kikkawa, *Microelectron. Eng.* **2011**, *88*, 666.
[39] H. J. Scheibe, B. Schultrich, *Thin Solid Films* **1994**, *246*, 92.
[40] F. Vaz, S. Carvalho, L. Rebouta, M. Z. Silva, A. Paúl, D. Schneider, *Thin Solid Films* **2002**, *408*, 160.
[41] G. Chow, E. Uchaker, G. Cao, J. Wang, *Mech. Mater.* **2015**, *91*, 333.
[42] L. Q. Chu, W. Knoll, R. Förch, *Langmuir* **2006**, *22*, 5548.
[43] M. K. Baller, H. P. Lang, J. Fritz, C. Gerber, J. K. Gimzewski, U. Drechsler, H. Rothuizen, M. Despont, P. Vettiger, F. M. Battiston, J. P. Ramseyer, P. Fornaro, E. Meyer, H.-J. Güntherodt, *Ultramicroscopy* **2000**, *82*, 1.
[44] N. Vandencasteele, F. Reniers, *J. Electron. Spectrosc. Relat. Phenom.* **2010**, *178*, 394.
[45] M. S. Silverstein, L. Sandrin, E. Sacher, *Polymer* **2001**, *42*, 4299.
[46] M. Toda, Y. Joseph, R. Berger, *Journal of Physical Chemistry C* **2010**, *114*, 2012.
[47] J. R. Barnes, R. J. Stephenson, C. N. Woodburn, S. J. O'Shea, M. E. Welland, T. Rayment, J. K. Gimzewski, C. Gerber, *Rev. Sci. Instrum.* **1994**, *65*, 3793.
[48] R. Raiteri, M. Grattarola, H.-J. Butt, P. Skládal, *Sensors and Actuators B: Chemical* **2001**, *79*, 115.
[49] A. N. Itakura, M. Toda, K. Miyake, R. Förch, R. Berger, *Japanese Journal of Applied Physics* **2013**, *52*, 110111.
[50] C. Li, Z. Huang, R. K. Wang, *Opt. Express* **2011**, *19*, 10153.
[51] A. Neubrand, P. Hess, *J. Appl. Phys.* **1992**, *71*, 227.
[52] C. Sun, B. Standish, V. X. Yang, *J Biomed Opt* **2011**, *16*, 043001.
[53] D. Schneider, T. Schwarz, *Surf. Coat. Technol.* **1997**, *91*, 136.
[54] G. Stoney, *Proceedings of the Royal Society of London. Series A*, **1909**, 172.
[55] M. Toda, A. N. Itakura, S. Igarashi, K. Buscher, J. S. Gutmann, K. Graf, R. Berger, *Langmuir* **2008**, *24*, 3191.
[56] R. C. Cammarata, *Prog. Surf. Sci.* **1994**, *46*, 1.
[57] M. Mizusawa, K. N. Stoev, K. Sakurai, *Japanese Journal of Applied Physics* **2003**, *42*, 3709.
[58] S. Sakata, Y. Inoue, K. Ishihara, *Transactions of the Materials Research Society of Japan* **2016**, *41*, 51.
[59] J. E. Mark, "*Polymer Data Handbook*", Oxford University Press, 1999.
[60] S. S. Bedair, G. K. Fedder, *Transducers '05, Digest of Technical Papers, Vols 1 and 2* **2005**, 2035.
[61] R. Zhang, T. Cherdhirankorn, K. Graf, K. Koynov, R. Berger, *Microelectron. Eng.* **2008**, *85*, 1261.

Figures

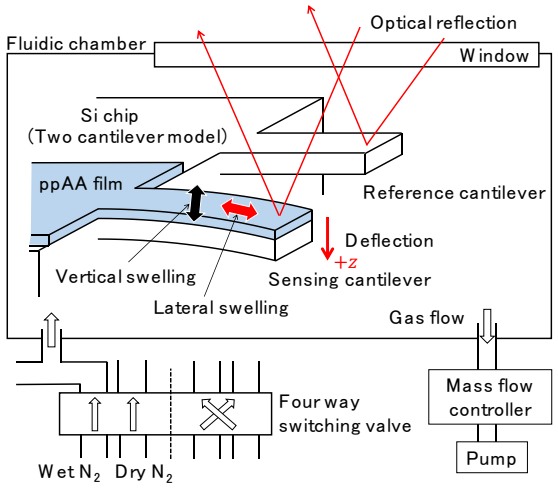

Figure 1. This schematic diagram shows the principle of the MCS bending technique. The deflection is measured along the +z direction. Here, the lateral swelling (red arrow) of polymer film deposited on top of the MCS along the beam direction results in a bending of MCS.

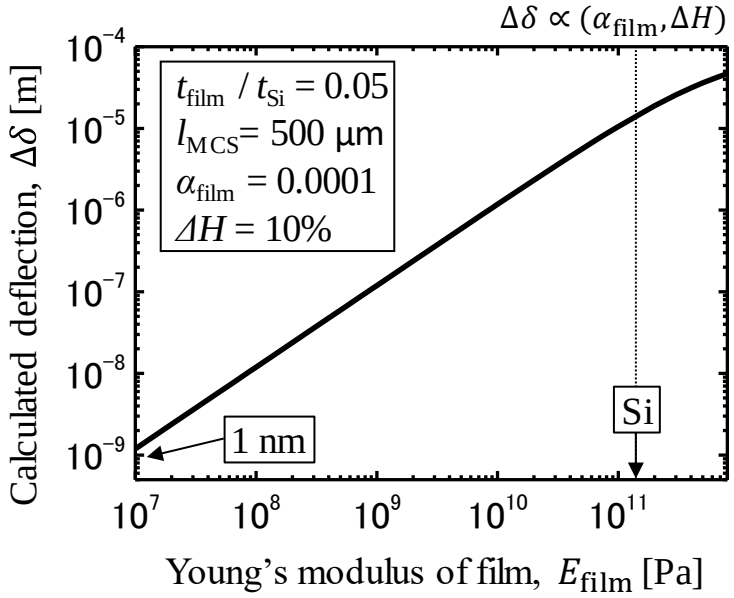

Figure 2. Calculated Young's modulus of a thin uniform polymer film (t_{film} = 100 nm) that is located on a 500 µm long MCS made from silicon (t_{Si} = 2 µm). The deflection is induced by a humidity change ΔH of 10 % while a constant expansion coefficient α_{film} is assumed.

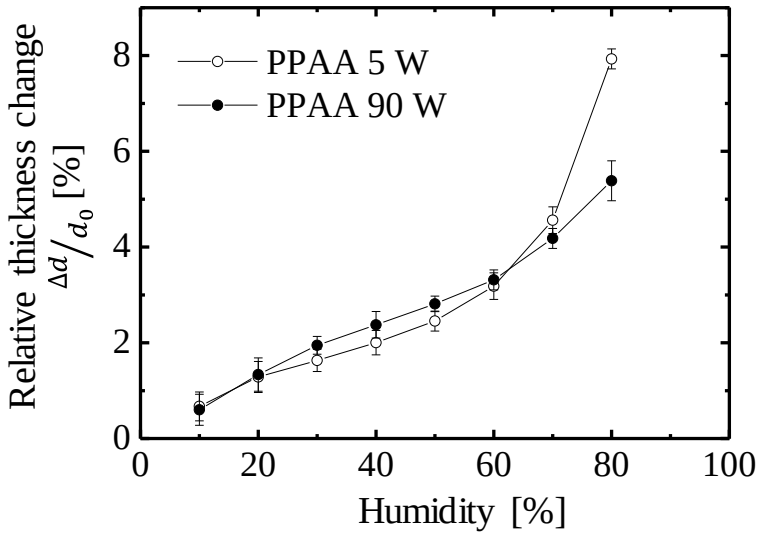

Figure 3 (a). The relative film thickness change, i.e. ($\Delta d/d_0$), of ppAA films prepared with 5 W and 90 W plasma power levels as a function of humidity. Δd and d_0 are the changes in the thickness and the thickness at 0 % humidity, respectively.

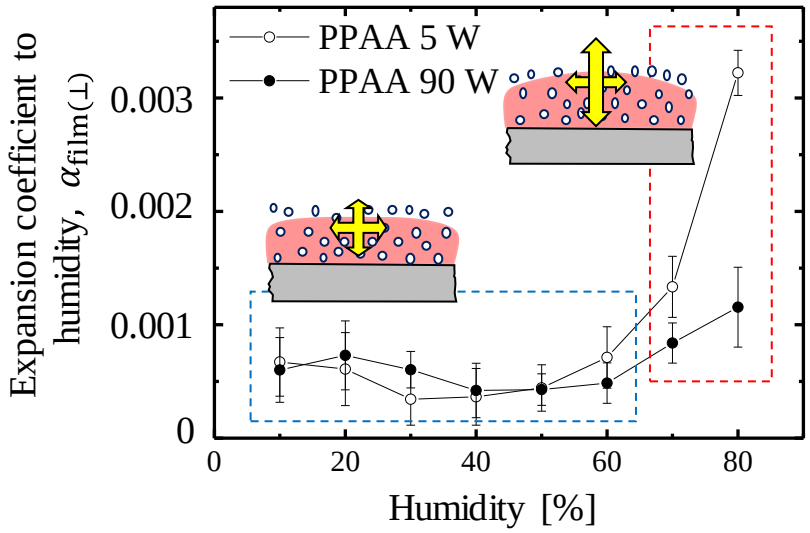

Figure 3 (b). Calculated expansion coefficients of ppAA films. Ellipsometry measurements indicated that the expansion coefficient at H < 60 % is constant (blue dashed line). This can indicate isotropic swelling (yellow arrows). At H > 70 %, the measured $\alpha_{film\ \perp}$ increased up to six times for the 5 W ppAA film and two times for the 90 W ppAA film (red dashed line). Here it possibly indicates hindrance in lateral expansions while vertical expansion is promoted. This is depicted by different sized yellow arrows.

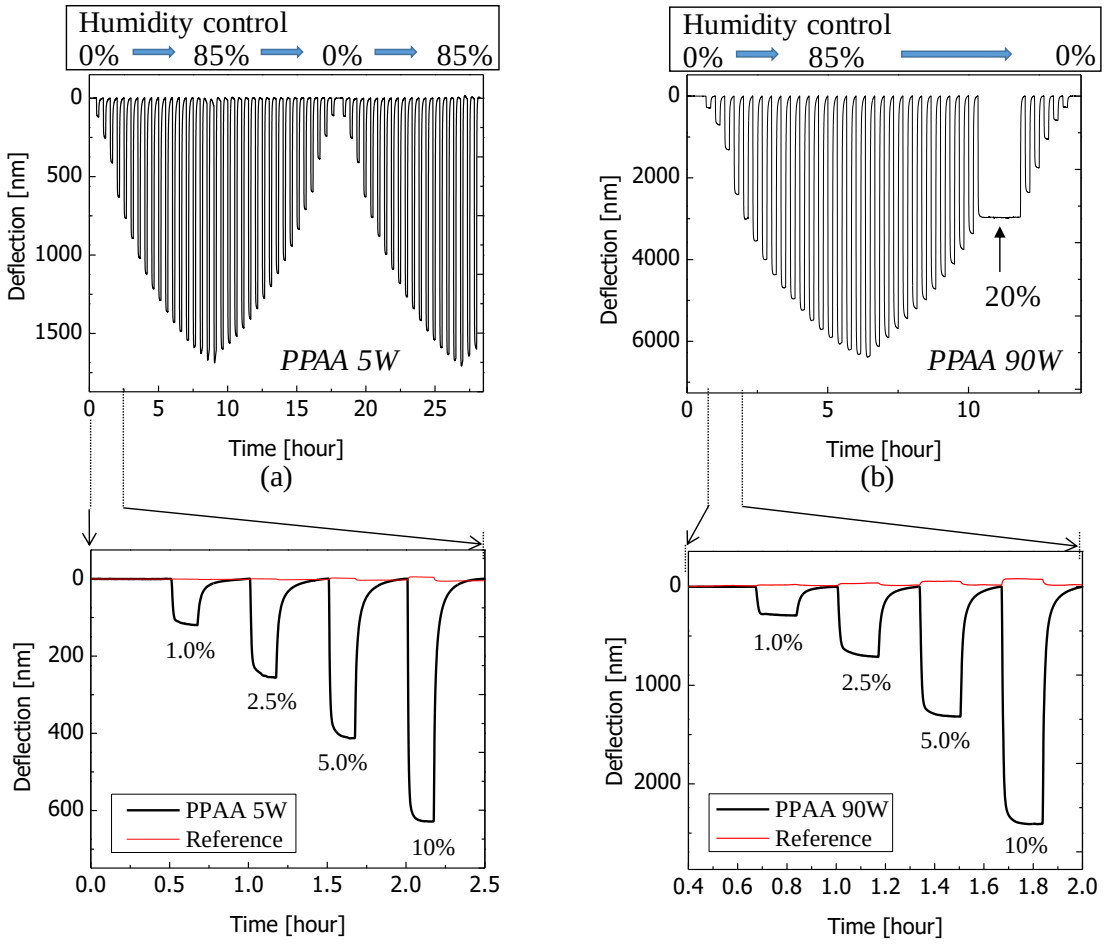

Figure 4. Series of exposures of the MCSs coated with ppAA films at different humidities. The MCSs were exposed alternatively to each defined humidity value followed by exposure to dry nitrogen. Switching the 4-way solenoid valve allowed rapid changes (< 100 msec) of flow in the sample cell between 0 % humidity and different levels of humidity. One complete cycle of increasing and decreasing humidity was performed in 18 hours. (a, c) ppAA films deposited with 5 W and (b, d) 90 W plasma power.

493

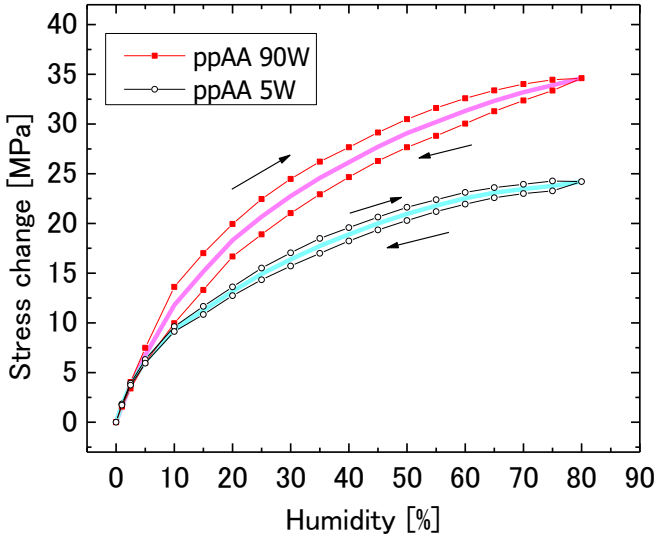

494 *Figure 5. Saturated surface stress in compressive responses at each stage of humid environment*

495 *for ppAA films. The black arrows indicate increasing and decreasing humidity cycles. The solid*

496 *green and pink lines correspond to the average stress changes calculated from increasing and*

497 *decreasing humidity cycles.*

498

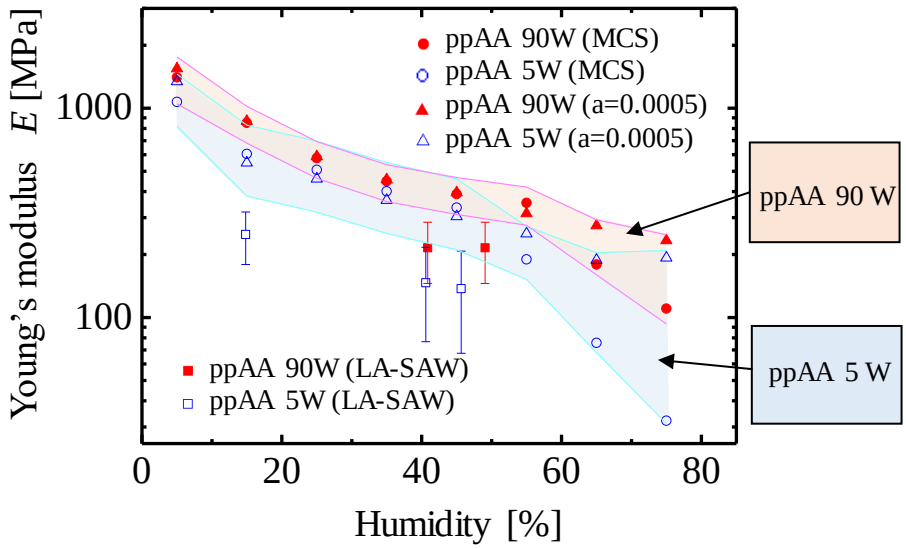

499

500 *Figure 6. The calculated Young's modulus using the MCS (circles and triangles) and the LA-*
501 *SAW (squares) techniques. The uncertainininty in E_{film} values for the MCS technique is dominated*
502 *by the error in α_{film}, which was calculated from the thickness measurements by ellipsometry at*
503 *different humidities. The error bars for the LA-SAW measurement correspond to measurements*
504 *at different points on the sample and different distances Δl. An error of ±3 % in the humidity*
505 *values based on the stability of the humidity of the measurement system during the experiments*
506 *was calculated in. In total, we obtained error bars of 0.07 GPa in the value of E'_{film}.*

507